THE JOURNAL OF PHYSICAL CHEMISTRY A

Article

Cite This: J. Phys. Chem. A 2019, 123, 9292−9297

pubs.acs.org/JPCA

Effect of Reaction Parameters on the Wavelength of Pulse Waves in the Belousov−Zhabotinsky Reaction−Diffusion System

Rui Teng,[†] Lin Ren,[†] Ling Yuan,[†] Liyuan Wang,[†] Qingyu Gao,*[,†] and Irving R. Epstein*[,‡]

[†]College of Chemical Engineering, China University of Mining and Technology, Xuzhou 221008, Jiangsu, P. R. China

[‡]Department of Chemistry and Volen Center for Complex Systems, Brandeis University, Waltham, Massachusetts 02454-9110, United States

ABSTRACT: The wavelength of Belousov−Zhabotinsky (BZ) traveling waves is the key factor that limits the scale of BZ self-oscillating gel motors. To achieve control of the wavelength, it is necessary to evaluate the wavelength dependence on species concentrations and temperature. In this work, the effect of reaction parameters on the wavelength of BZ pulse waves was studied. The most effective way to reduce the wavelength of pulse waves is to increase the concentration of organic species and/or the temperature. Decreasing the concentration of bromate, hydrogen ion, or metal catalyst also reduces the wavelength of pulse waves. This work provides a convenient and direct method to produce sub-millimeter BZ waves, which could be applied to designing BZ wave-driven small-scale gel motors as well as providing insight into other emergent behaviors of self-oscillating gels.

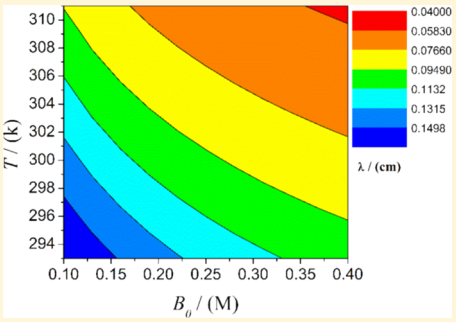

INTRODUCTION

Active soft matter[1,2] is able to convert free energy into systematic deformation and motion. In some cases, such as Janus particles,[3] the direction of motion is difficult to control without an external field gradient. This problem can be solved in Belousov−Zhabotinsky (BZ) self-oscillating gels, which generate locomotion driven by stable traveling waves. By adjusting the kinetic parameters of chemical waves, various modes of locomotion can be obtained.[4−8] In nature, the locomotion of jellyfish[9] and earthworms[10] propelled by waves of neural impulses has the same dynamical origin as that of a BZ self-oscillating gel driven by chemical waves. The universality and controllability of BZ gels makes them an ideal vehicle to study the basic locomotion behavior of bionic robots. However, the need for the gel to be able to host at least one full wavelength of the chemical waves places a lower limit on the size of the objects that can be studied. BZ-Ru(II) waves typically have a wavelength greater than 0.2 cm,[11] which implies that they can only generate locomotion in BZ gels whose length exceeds this value. To build small-scale gel motors, it is essential to shorten the chemical wavelength. We ask here to what extent one can decrease the BZ wavelength, thereby making it possible to build smaller-scale gel motors for studying collective behavior,[12] self-organization,[13] and micro soft robots.[14] Although one can use pacemakers to shorten the chemical wavelength,[11] this approach requires devoting a large part of the gel to the pacemaker, which increases the size of the gel and is not suitable for small-scale gel motors. Therefore, we employ the easily controllable parameters, concentration and temperature, as the means to achieve wavelength reduction.

Reaction−diffusion (RD) traveling waves have frequently been studied in the BZ reaction since, by virtue of its ability to oscillate in a closed system for many hours, it has become the prototype system for investigating spatiotemporal complexity in chemistry. Field[15] determined the relationship between the reactant and catalyst concentrations and the velocity of BZ waves. Tyson[16] studied the dispersion of traveling waves in the BZ reaction. Yoshida[17] studied the effect of the reactant concentrations on the oscillation period, waveform, and induction period in BZ self-oscillating gels.

In this paper, we numerically study the effect of modest concentration and temperature variations on the pulse wavelength and waveform in the BZ reaction in a one-dimensional reaction−diffusion system. The concentration variation, starting from the values typically used in experiments, is less than one order of magnitude, and the temperature range is 20 °C. Our initial aim was to find a parameter region in which the wavelength is less than 1 mm. In fact, with the convenient and direct method described here, i.e., adjusting the reaction concentrations and temperature, the minimum wavelength we obtained was 0.04 cm, which would allow for the development of significantly smaller-scale BZ gel motors.

MECHANISTIC MODEL AND METHOD

Our numerical simulations are based on an improved five-variable Oregonator-class model.[18] Here, the concentration of bromomalonic acid is considered to be approximately constant and the photosensitive effect is also ignored. The mechanistic model can be expressed in the following form

Received: August 30, 2019
Revised: October 1, 2019
Published: October 3, 2019

DOI: 10.1021/acs.jpca.9b08254
J. Phys. Chem. A 2019, 123, 9292−9297

$$A + Y + 2H \rightarrow X + P \quad (O1)$$

$$X + Y + H \rightarrow 2P \quad (O2)$$

$$A + X + H \rightarrow 2W \quad (O3)$$

$$2W \rightarrow A + X + H \quad (O4)$$

$$M_{re} + W + H \rightarrow X + M_{ox} \quad (O5)$$

$$2X \rightarrow A + P + H \quad (O6)$$

$$M_{ox} + B \rightarrow hY \quad (O7)$$

The model differs from the original Oregonator model[19] by taking explicit account of the concentration of reduced catalyst and introducing the radical BrO_2 (W), which allows us to take the total concentration of metal ions into account. To achieve these aims, we introduce three steps (O3, O4, O5) involving the autocatalyst BrO_2 and the reduced catalyst $Ru(bipy)_3^{2+}$, which are detailed in Amemiya's work on the $Ru(bipy)_3$-catalyzed BZ reaction.[18] A, B, H, P, X, Y, M_{re}, and M_{ox} denote the species BrO_3^-, total organic matter, H^+, HBrO, $HBrO_2$, Br^-, reduced catalyst, and oxidized catalyst, respectively. The total catalyst concentration, C_0, is constant, i.e., $[M_{ox}] + [M_{re}] = [C_0]$, so $[M_{re}]$ can be replaced by $[C_0] - [M_{ox}]$. The model assumes that the concentrations of A, H^+, and B are constant, so the corresponding partial differential equations (PDEs) reduce to a four-variable model

$$\frac{\partial X}{\partial t} = k_1 H_0^2 A_0 Y - k_2 H_0 XY - k_3 H_0 A_0 X + k_4 W^2 + k_5 H_0 (C_0 - M_{ox}) W - 2k_6 X^2 + D_X \frac{d^2 X}{dx^2}$$

$$\frac{\partial M_{ox}}{\partial t} = k_5 H_0 (C_0 - M_{ox}) W - k_7 B_0 M_{ox} + D_M \frac{d^2 M_{ox}}{dx^2}$$

$$\frac{\partial Y}{\partial t} = -k_1 H_0^2 A_0 Y - k_2 H_0 XY + hk_7 B_0 M_{ox} + D_Y \frac{d^2 Y}{dx^2}$$

$$\frac{\partial W}{\partial t} = 2k_3 H_0 A_0 X - 2k_4 W^2 - k_5 H_0 (C_0 - M_{ox}) W + D_W \frac{d^2 W}{dx^2} \quad (1)$$

where D_X, D_M, D_Y, and D_W are the diffusion coefficients of X ($HBrO_2$), M_{ox} (oxidized catalyst), Y (Br^-), and $BrO_2 \cdot (W)$, respectively. Here, we use $D_X = 1.5 \times 10^{-5}$ cm^2 s^{-1},[20] the experimentally determined diffusion coefficient of the autocatalyst, and we assume for simplicity that $D_Y = D_W = D_X$. The diffusion coefficient of the catalyst, D_M, is set to 0 to take into account that the catalyst is fixed in the BZ gel. Because we make only relatively modest changes in temperature, we neglect any effect of temperature on the diffusion coefficients. The simulation is implemented on a one-dimensional region of length 0.774 cm, which is sufficient to capture the propagation of chemical waves.

To solve the PDEs, we employ a fourth-order Runge−Kutta method with time step $\Delta t = 0.0001$ s. We discard the first 1×10^7 steps and use the subsequent 4×10^7 steps to characterize the oscillations. The default initial concentrations are $A_0 = 0.1$ M, $B_0 = 0.1$ M, $H_0 = 0.7$ M, and $C_0 = 0.5$ mM, respectively. The rate constants $k_1 - k_5$ are chosen according to the work of Amemiya[18] as $k_1 = 2.0$ M^{-3} s^{-1}, $k_2 = 3.0 \times 10^6$ M^{-2} s^{-1}, $k_3 = 42.0$ M^{-2} s^{-1}, $k_4 = 4.2 \times 10^7$ M^{-1} s^{-1}, $k_5 = 8 \times 10^6$ M^{-2} s^{-1}, and $k_6 = 3000$ M^{-1} s^{-1}. The value of $k_7 = 1$ M^{-1} s^{-1} is based on the work of Showalter.[21] The stoichiometric factor, $h = 0.6$, is a parameter that characterizes the BZ reaction.

The Arrhenius equation is used to estimate the rate constants at different temperatures. The rate constant $k_i(T)$ at temperature T can be calculated as

$$k_i(T) = k_i(T_0) \times e^{-(E_a(i)/R \times (1/T - 1/T_0))} \quad (2)$$

where $k_i(T_0)$, R, $E_a(i)$, and T_0 denote the rate constant at 293 K, molar gas constant ($R = 8.314$ J/mol·K), activation energy, and reference temperature (293 K), respectively. The activation energies are based on the work of Strizhak[22] and Koch,[23] where $E_1 = 54.0$, $E_2 = 25.4$, $E_3 = 23.0$, $E_4 = 0.0$, $E_5 = 0.0$, $E_6 = 23.0$, and $E_7 = 70.0$ kJ/ mol.

A stable chemical wave is generated by setting a fixed boundary value of X_0 ($HBrO_2$) at the left boundary, consistent with Luo's experiment.[24] This fixed-boundary value determines the wavelength of the excited chemical wave. To make sure our setting is reasonable and to establish a suitable value of X_0, we first obtain the dispersion relationship for the BZ reaction. The fixed boundary condition X_0 is changed from 1×10^{-7} to 1×10^{-4} M, yielding the relationship between wave velocity and wavelength shown in Figure 1. The wave velocity increases monotonically with wavelength, and the slope gradually decreases, showing a normal dispersion relationship. The dispersion relationship allows us to choose $X_0 = 3 \times 10^{-5}$ M as the fixed boundary value in our simulations, which gives a wavelength of about 0.150 cm.

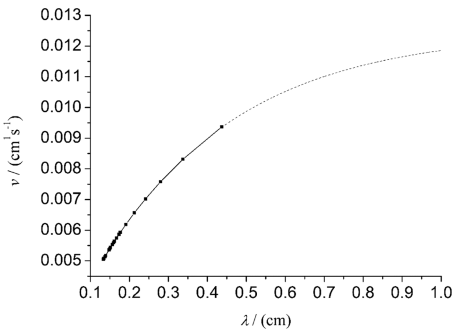

Figure 1. Relationship between wave velocity and wavelength. The dashed line is an extrapolation. Parameters are default values.

RESULTS AND DISCUSSION

Effect of Species Concentration on Wavelength. The wavelength (λ) of our chemical waves is calculated as the product of the period and velocity. First, we study the effect of B_0, A_0, H_0, and C_0, which are the controllable parameters in the experiment. Fixing the other parameters at their default values, we successively vary B_0, A_0, H_0, and C_0 to obtain the wavelength variation curves in Figure 2. On varying B_0 from 0.1 to 0.4 M (Figure 2a), λ decreases monotonically with B_0. The wavelength variation curve of A_0 is plotted in Figure 2b. As A_0 increases (Figure 2b), λ first decreases and then increases, reaching a minimum at about 0.05 M. In contrast to the effect of B_0, the wavelength increases monotonically with H_0 (Figure 2c). The effect of the catalyst concentration, C_0, on wavelength is shown in Figure 2d, where with increasing C_0, the wavelength rises almost linearly. A similar dependence of wavelength on A_0, B_0, H_0, and C_0 was observed in experiments by Bordyugov[25] and Nagy-Ungvarai[26] under quite different

DOI: 10.1021/acs.jpca.9b08254
J. Phys. Chem. A 2019, 123, 9292−9297

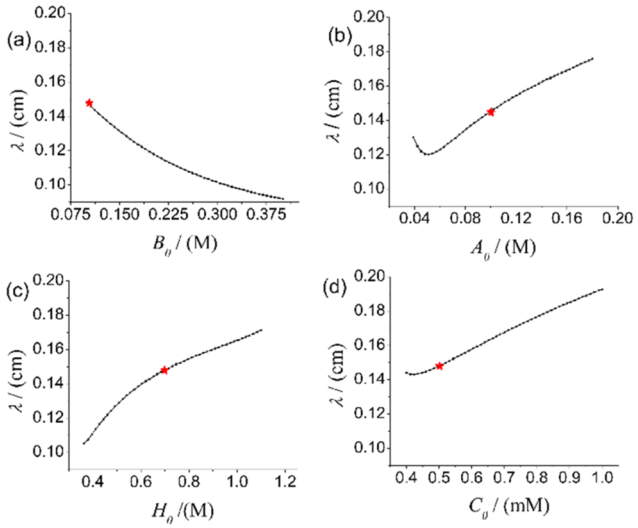

Figure 2. Effect of species concentrations on pulse wavelength. Other parameters are default values. The default values on each curve are marked by red stars. (a) Initial concentration of total organic matter (B_0). (b) Initial concentration of bromate (A_0). (c) Initial concentration of hydrogen ion (H_0). (d) Metal catalyst concentration (C_0).

reaction conditions, with a different catalyst and concentrations A_0, B_0, and H_0 higher than those used in our simulations.

It can be seen from Figure 2 that changing B_0 has the greatest effect on reducing the wavelength. Increasing B_0 can reduce the wavelength to 0.091 cm. Reducing A_0 and H_0 does not decrease the wavelength to less than 0.1 cm. Note that when A_0 or H_0 is too small, stable pulses cannot be generated. C_0 has the least effect on wavelength reduction and shows a minimum in λ of about 0.145 cm between C_0 = 0.40 and 0.50 mM. We discuss these observations further below when we analyze how the concentrations affect the wave velocity and oscillatory period.

Effect of Temperature. Since the above results indicate that the wavelength cannot be reduced significantly below the millimeter scale by changing the initial concentrations alone, we next consider the effect of temperature. In homogeneous systems, Bánsági et al.[27] have studied the relationship between the oscillatory frequency of the BZ reaction and temperature and obtained high-frequency oscillations by heating. A similar process can be envisioned in the RD system, with a decrease in wavelength resulting from a shortening of the period (increase in frequency) due to the temperature rise. This notion is confirmed in our simulation. Figure 3 shows how the wavelength decreases nearly linearly with temperature under the default conditions, falling to 0.082 cm at 311 K.

By varying both the temperature and the species concentrations, we can change the wavelength over a still wider range. To better describe the variation of wavelength and find the optimal region of small wavelength parameters, we studied the parametric variation of the wavelength. Fixing C_0 at its default value, we plot in Figure 4 the distribution of wavelengths in the A_0–H_0–B_0 parameter space at four different temperatures. Figure 4a shows the parameter space distribution of wavelength at 293 K. When B_0 = 0.1 M, a complex spatiotemporal oscillatory region (gray, cp) appears in the A_0–H_0 plane at low A_0 and H_0. In this region, pulse waves are unstable and cannot be transmitted continuously.

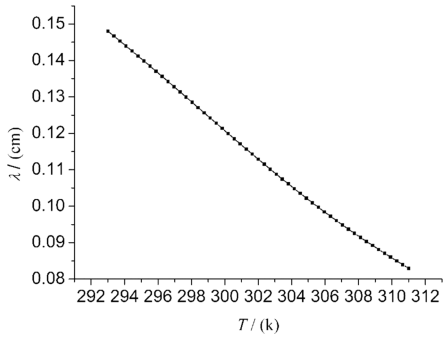

Figure 3. Effect of temperature (T) on pulse wavelength at default concentrations.

In the simple pulse region, the contours of constant wavelength form smooth arcs in each A_0–H_0 plane at fixed B_0. The region just to the right of the complex oscillatory (gray) region contains the smallest wavelengths. With increasing B_0, the wavelength decreases in each A_0–H_0 plane, while the qualitative pattern remains the same. At the highest temperature we studied, 311 K, we obtain a minimum wavelength of 0.04 cm, which is much smaller than the maximum wavelength of 0.27 cm at 293 K. Thus, the wavelength of BZ chemical waves can be significantly reduced by adjusting the temperature and the three reactant concentrations. As the temperature and B_0 increase, the complex spatiotemporal region expands. Meanwhile, the nonoscillatory region (black) occurs at low A_0 and H_0.

Analysis of Dependence of Wavelength on Parameters. We now consider the relationship between wave velocity, oscillatory period, wavelength, and the three reactant concentrations, to which the wavelength is more sensitive than to the catalyst concentration. In general, the wavelength is given by $\lambda = v \times P$, where v is the wave velocity and P is the oscillatory period. Thus, to reduce the wavelength, we must decrease v and/or P. However, v and P tend to move in opposite directions as the parameters are varied. To analyze the wavelength variation, we plot the period and wave velocity under the same conditions as in Figure 2, varying B_0, A_0, and H_0. The dependences of the wavelength, wave velocity, and oscillatory period on these three reactants are consistent with previous studies.[20,28]

As shown in Figure 5a, v varies only very slightly with B_0, while P decreases monotonically with B_0. The change of wavelength is thus governed solely by the decrease in the period. Unlike the effect of changing B_0, the wave velocity increases significantly with A_0 (Figure 5b), while P decreases monotonically with a decreasing slope. Of the three reactant concentrations, A_0 has the most pronounced effect on P. The competition between the falling P and the rising v as A_0 increases is responsible for the minimum found in the λ versus A_0 curve in Figure 2b. A similar effect accounts for the similar but a much shallower minimum in the λ–H_0 curve (see Figures 2d and 5c).

Relationship between Wavelength and Waveform. The waveform of the chemical wave is of great significance to the locomotion of BZ gels, since it determines the push–pull forces that determine the direction of motion.[7] In RD systems, various waveforms can be obtained when the reaction solution has different oxidative and reductive compositions.[29,30] In Figure 6, we examine the effect of B_0, A_0, H_0, and T on the waveform of the BZ system studied here. Each panel in Figure

DOI: 10.1021/acs.jpca.9b08254
J. Phys. Chem. A 2019, 123, 9292–9297

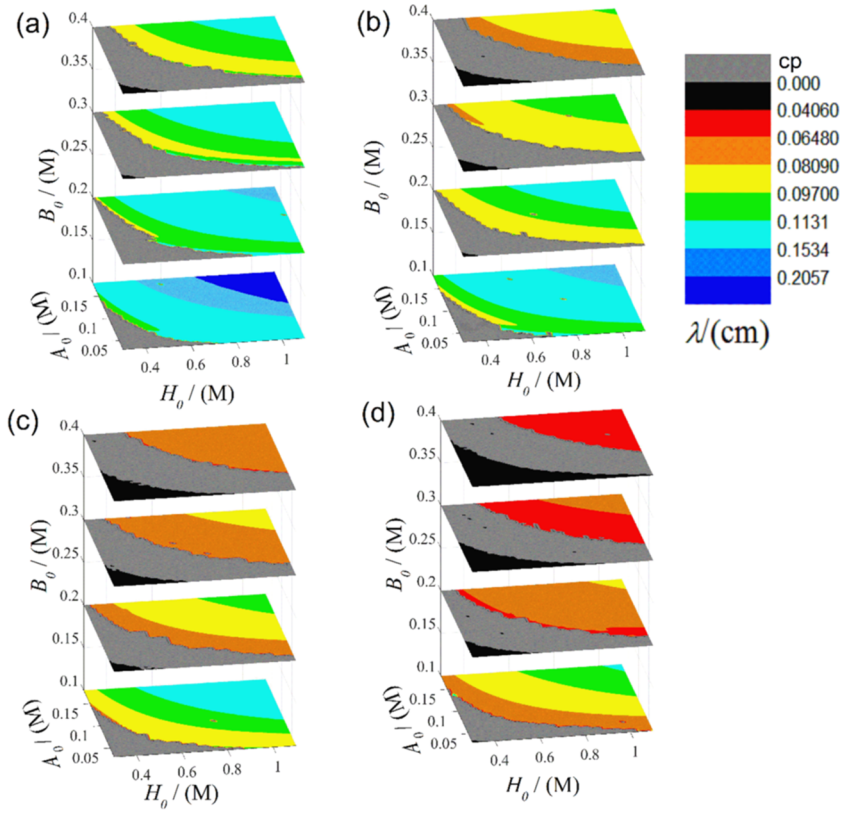

Figure 4. Wavelength dependence on reactant concentrations at several temperatures. Catalyst concentration is default value. (a) T = 293 K; (b) T = 299 K; (c) T = 305 K; and (d) T = 311 K. cp = complex behavior with no simple pulse waves. No oscillations occur in the black regions.

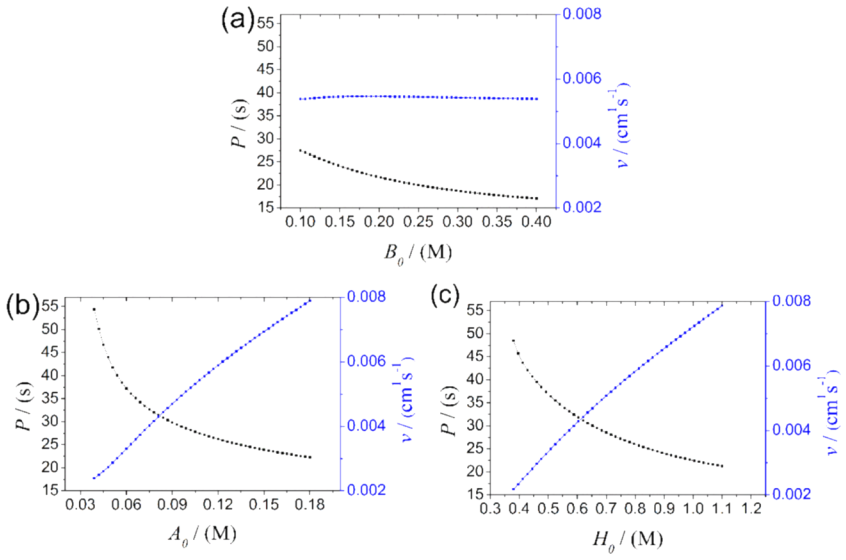

Figure 5. Effect of substrate concentrations on wave velocity (v) and oscillatory period (P). Other parameters are default values. (a) Initial concentration of total organic matter (B_0). (b) Initial concentration of bromate (A_0). (c) Initial concentration of hydrogen ion (H_0).

6 is the stationary oscillatory waveform (concentration of oxidized catalyst vs position) recorded after 1×10^7 time steps to ensure the stability of the waveform. For convenience of comparison, in each trio of panels, one parameter is changed, while the others are fixed at their default values.

The waveforms in Figure 6 help to explain the wavelength decrease with B_0 and temperature and increase with A_0 and H_0 described earlier. In each curve, the wavefront rises rapidly and then reaches a plateau. Varying a reactant concentration or the temperature changes the waveback slope and the peak width. Figure 6a shows the waveform for varying B_0. With increasing B_0, the width of the plateau decreases and the slope of the waveback increases, thereby decreasing the wavelength. The change in the waveform can be understood in terms of our BZ mechanistic model. As described in the model, the change of the amount of oxidized catalyst results from the formation step O5 and the consumption step O7. An increase in B_0 benefits O7, which leads to a faster consumption of oxidized catalyst,

DOI: 10.1021/acs.jpca.9b08254
J. Phys. Chem. A 2019, 123, 9292−9297

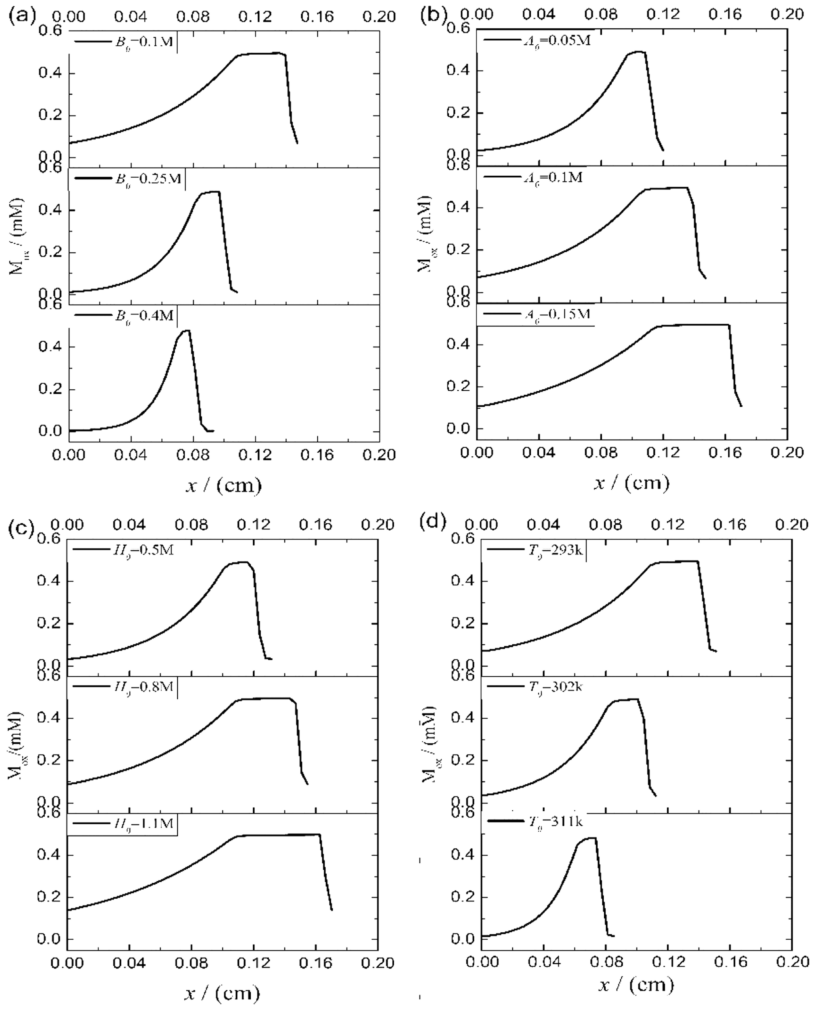

Figure 6. Effect of parameters on pulse waveform. Other parameters are default values: (a) A_0, (b) B_0, (c) H_0, and (d) T.

narrowing the peak width and accelerating the decline of the waveback. A similar waveform evolution is observed with increasing temperature (Figure 6d) and can be explained by a similar mechanism. When the temperature rises, the rate constant of step O7 increases, leading to a more rapid consumption of oxidized catalyst. The waveform changes with increasing A_0 and H_0 plotted in Figure 6b,c show an increase of the peak width with increasing concentration. Here, increasing A_0 or H_0 promotes the production of the radical BrO_2, thus enabling step O5 to maintain the maximum concentration of oxidized catalyst for a longer interval.

CONCLUSIONS

We have studied the variation of wavelength in a model RD BZ system with species concentration and temperature. The numerical results reveal that increasing the temperature and initial concentration of total organic matter can significantly reduce the wavelength. Increasing the initial concentrations of bromate or hydrogen ions and the catalyst concentration will make the wavelength longer. Moreover, as the species concentrations and temperature change, the chemical waveform also changes. Increasing the initial concentration of malonic acid and reaction temperature narrows the wave peak, while bromate and hydrogen ions have the opposite effect on peak width.

It is important to reiterate that reducing the length of the chemical wave is a prerequisite to develop smaller-scale BZ gel motors. In our study, the wavelength has been reduced by nearly one order of magnitude under mild reaction conditions. The minimum wavelength we have found is 0.04 cm. Further reducing the wavelength by additional temperature increases may not be feasible because doing so will shorten the oscillatory lifetime.[27] However, the results in this work are based on rate constants for the $Ru(bipy)_3^{2+}$-catalyzed BZ system,[18,21] and it is likely that if $Fe(phen)_3^{2+}$ or $Fe(bip)_3^{2+}$ rather than Ru(III)/Ru(II) used as the catalyst, the wavelength could be further reduced,[25] since the rate constants of Reactions O5 and O7 would be changed (or the mechanism may need to be adjusted[31]). As progress continues toward motors driven by chemical reactions (e.g., pH or biochemical oscillators) in active gels, similar studies of the wavelength dependence on system parameters are likely to be needed.

AUTHOR INFORMATION

Corresponding Authors

*E-mail: gaoqy@cumt.edu.cn (Q.G.).
*E-mail: epstein@brandeis.edu (I.R.E.).

ORCID

Irving R. Epstein: 0000-0003-3180-4055

DOI: 10.1021/acs.jpca.9b08254
J. Phys. Chem. A 2019, 123, 9292−9297

Notes

The authors declare no competing financial interest.

■ ACKNOWLEDGMENTS

This work was supported by the National Natural Science Foundation of China (Grant Nos. 21573282 and 21972165), the Fundamental Research Funds for the Central Universities (Grant No. 2015XKMS045), and the U.S. National Science Foundation (Grant No. CHE-1856484).

■ REFERENCES

(1) Yoshida, R.; Takahashi, T.; Yamaguchi, T.; Ichijo, H. Self-oscillating gel. *J. Am. Chem. Soc.* **1996**, *118*, 5134−5135.
(2) Marchetti, M. C.; Joanny, J. F.; Ramaswamy, S.; Liverpool, T. B.; Prost, J.; Rao, M.; Simha, R. A. Hydrodynamics of soft active matter. *Rev. Mod. Phys.* **2013**, *85*, 1143−1189.
(3) Das, S.; Garg, A.; Campbell, A. I.; Howse, J.; Sen, A.; Velegol, D.; Golestanian, R.; Ramin, S. J. Boundaries can steer active Janus spheres. *Nat. Commun.* **2015**, *6*, No. 8999.
(4) Maeda, S.; Hara, Y.; Sakai, T.; Yoshida, R.; Hashimoto, S. Self-walking gel. *Adv. Mater.* **2007**, *19*, 3480−3484.
(5) Lu, X.; Ren, L.; Gao, Q.; Zhao, Y.; Wang, S.; Yang, J.; Epstein, I. R. Photophobic and phototropic movement of a self-oscillating gel. *Chem. Commun.* **2013**, *49*, 7690−7692.
(6) Ren, L.; She, W.; Gao, Q.; Pan, C.; Ji, C.; Epstein, I. R. Retrograde and direct wave locomotion in a photosensitive self-oscillating gel. *Angew. Chem., Int. Ed.* **2016**, *55*, 14301−14305.
(7) Ren, L.; Wang, M.; Pan, C.; Gao, Q.; Liu, Y.; Epstein, I. R. Autonomous reciprocating migration of an active material. *Proc. Natl. Acad. Sci. U.S.A.* **2017**, *114*, 8704−8709.
(8) Dayal, P.; Kuksenok, O.; Balazs, A. C. Reconfigurable assemblies of active, autochemotactic gels. *Proc. Natl. Acad. Sci. U.S.A.* **2013**, *110*, 431−436.
(9) Gemmell, B. J.; Costello, J. H.; Colin, S. P.; Stewart, C. J.; Dabiri, J. O.; Tafti, D.; Priya, S. Passive energy recapture in jellyfish contributes to propulsive advantage over other metazoans. *Proc. Natl. Acad. Sci. U.S.A.* **2013**, *110*, 17904−17909.
(10) Gray, J.; Lissmann, H. W. Studies In Animal Locomotion: VII. Locomotory Reflexes in The Earthworm. *J. Exp. Biol.* **1938**, *15*, 506−517.
(11) Mahara, H.; Saito, T.; Amagishi, Y.; Nagashima, H.; Yamaguchi, T. "Ring-Shaped Model" of the Pacemaker in Oscillatory Reaction-Diffusion System. *J. Phys. Soc. Jpn.* **2000**, *69*, 3552−3554.
(12) Li, S.; Batra, R.; Brown, D.; Chang, H. D.; Ranganathan, N.; Hoberman, C.; Rus, D.; Lipson, H. Particle robotics based on statistical mechanics of loosely coupled components. *Nature* **2019**, *567*, 361.
(13) Zhang, J.; Luijten, E.; Grzybowski, B. A.; Granick, S. Active colloids with collective mobility status and research opportunities. *Chem. Soc. Rev.* **2017**, *46*, 5551−5569.
(14) Hu, W.; Lum, G. Z.; Mastrangeli, M.; Sitti, M. Small-scale soft-bodied robot with multimodal locomotion. *Nature* **2018**, *554*, 81.
(15) Field, R. J.; Noyes, R. M. Oscillations in chemical systems. V. Quantitative explanation of band migration in the Belousov-Zhabotinskii reaction. *J. Am. Chem. Soc.* **1974**, *96*, 2001−2006.
(16) Dockery, J. D.; Keener, J. P.; Tyson, J. J. Dispersion of traveling waves in the Belousov-Zhabotinskii reaction. *Phys. D* **1988**, *30*, 177−191.
(17) Suzuki, D.; Yoshida, R. Effect of Initial Substrate Concentration of the Belousov− Zhabotinsky Reaction on Self-Oscillation for Microgel System. *J. Phys. Chem. B* **2008**, *112*, 12618−12624.
(18) Amemiya, T.; Yamamoto, T.; Ohmori, T.; Yamaguchi, T. Experimental and Model Studies of Oscillations, Photoinduced Transitions, and Steady States in the $Ru(bpy)_3^{2+}$-Catalyzed Belousov− Zhabotinsky Reaction under Different Solute Compositions. *J. Phys. Chem. A* **2002**, *106*, 612−620.
(19) Field, R. J.; Noyes, R. M. Oscillations in chemical systems. IV. Limit cycle behavior in a model of a real chemical reaction. *J. Chem. Phys.* **1974**, *60*, 1877−1884.
(20) Nagy-Ungvarai, Z.; Tyson, J. J.; Hess, B. Experimental study of the chemical waves in the cerium-catalyzed Belousov-Zhabotinskii reaction. 1. Velocity of trigger waves. *J. Phys. Chem. C* **1989**, *93*, 707−713.
(21) Kádár, S.; Amemiya, T.; Showalter, K. Reaction Mechanism for Light Sensitivity of the $Ru(bpy)_3^{2+}$-Catalyzed Belousov− Zhabotinsky Reaction. *J. Phys. Chem. A* **1997**, *101*, 8200−8206.
(22) Strizhak, P. E.; Didenko, O. Z. Analysis of the effect of temperature on complex self-oscillation regimes in the Belousov-Zhabotinskii reaction in a constant-agitation flow-through reactor. *Theor. Exp. Chem.* **1997**, *33*, 133−137.
(23) Koch, E.; Nagy-Ungvarai, Z. New strategies for studies on the kinetics and energetics of the Belousov-Zhabotinskii reaction. *Ber. Bunsenges. Phys. Chem.* **1987**, *91*, 1375−1386.
(24) Luo, H.; Wang, C.; Ren, L.; Gao, Q.; Pan, C.; Epstein, I. R. Light-Modulated Intermittent Wave Groups in a Diffusively Fed Reactive Gel. *Angew. Chem.* **2016**, *128*, 5072−5075.
(25) Bordyugov, G.; Fischer, N.; Engel, H.; Manz, N.; Steinbock, O. Anomalous dispersion in the Belousov−Zhabotinsky reaction: Experiments and modeling. *Phys. D* **2010**, *239*, 766−775.
(26) Nagy-Ungvarai, Z.; Mueller, S. C.; Tyson, J. J.; Hess, B. Experimental study of the chemical waves in the cerium-catalyzed Belousov-Zhabotinskii reaction. 2. Concentration profiles. *J. Phys. Chem. C* **1989**, *93*, 2760−2764.
(27) Bánsági, T., Jr.; Leda, M.; Toiya, M.; Zhabotinsky, A. M.; Epstein, I. R. High-frequency oscillations in the Belousov-Zhabotinsky reaction. *J. Phys. Chem. A* **2009**, *113*, 5644−5648.
(28) Ren, L.; Fan, B.; Gao, Q.; Zhao, Y.; Luo, H.; Xia, Y.; Lu, X.; Epstein, I. R. Experimental, numerical, and mechanistic analysis of the nonmonotonic relationship between oscillatory frequency and photointensity for the photosensitive Belousov−Zhabotinsky oscillator. *Chaos* **2015**, *25*, No. 064607.
(29) Zhabotinsky, A. M.; Buchholtz, F.; Kiyatkin, A. B.; Epstein, I. R. Oscillations and waves in metal-ion-catalyzed bromate oscillating reactions in highly oxidized states. *J. Phys. Chem. C* **1993**, *97*, 7578−7584.
(30) Masuda, T.; Akimoto, A. M.; Furusawa, M.; Tamate, R.; Nagase, K.; Okano, T.; Yoshida, R. Aspects of the Belousov−Zhabotinsky Reaction inside a Self-Oscillating Polymer Brush. *Langmuir* **2018**, *34*, 1673−1680.
(31) Wang, J.; Zhao, J.; Chen, Y.; Gao, Q.; Wang, Y. Coexistence of Two Bifurcation Regimes in a Closed Ferroin-Catalyzed Belousov−Zhabotinsky Reaction. *J. Phys. Chem. A* **2005**, *109*, 1374−1381.

DOI: 10.1021/acs.jpca.9b08254
J. Phys. Chem. A 2019, 123, 9292−9297